Optimization of Weighted Curvature for Image Segmentation

Noha El-Zehiry and Leo Grady

Department of Image Analytics and Informatics
Siemens Corporate Research
Princeton, NJ

Abstract. Minimization of boundary curvature is a classic regularization technique for image segmentation in the presence of noisy image data. Techniques for minimizing curvature have historically been derived from descent methods which could be trapped in a local minimum and therefore required a good initialization. Recently, combinatorial optimization techniques have been applied to the optimization of curvature which provide a solution that achieves nearly a global optimum. However, when applied to image segmentation these methods required a meaningful data term. Unfortunately, for many images, particularly medical images, it is difficult to find a meaningful data term. Therefore, we propose to remove the data term completely and instead *weight* the curvature locally, while still achieving a global optimum.

1 Introduction

A classic prior model for the boundary of objects in an image is that the boundary have a small curvature. This model was proposed and theoretically justified by Mumford [1] and also appeared in the first active contour work by Kass, Witkin and Terzopoulos [2] who proposed an optimization of the boundary curvature. Subsequently, the optimization of boundary curvature became a common feature of variational methods for active contours and level sets [3,4,5]. However, all of these methods use descent-based optimization, causing the solution to get stuck in a local minimum and depend strongly on having a good initialization. Following the description by Bruckstein *et al.* [6] of the curvature of a polygon, the curvature of an object boundary was formulated on a graph by Schoenneman *et al.* [7] (and previously in a different manner by the same authors [8]). Specifically, on the graph *dual* to the pixel lattice, the boundary of an object may be described by a polygon comprised of graph edges, and therefore the boundary having minimum curvature could be found by optimizing over all polygons which had a curvature value as defined by Bruckstein *et al.*. However, this optimization required a long computation time (minutes to hours) and often did not find a solution achieving a global optimum. Therefore, this work was followed by El-Zehiry and Grady [9] who used a *primal* formulation of the curvature energy that parameterized the boundary polygon in terms of the normal vectors and computed a solution in seconds which often achieved a global optimum. For simplicity, in this work we consider only the segmentation of an object from a background, i.e., a two-class image segmentation problem.

All of these previous approaches to utilizing curvature minimization employed curvature as a boundary *regularization* for a data term which modeled the object and background intensity/color/texture/etc. Since this data term was imperfect (due to noise), the curvature regularization was used to regularize the solution. However, in practice, this approach can suffer from two problems: 1) It may be hard to model the object and background data *a priori* or, worse, the distributions can significantly overlap (or even be equal), 2) Sometimes the true object boundary has a high curvature, but a minimum curvature regularization can cause the boundary to become erroneously smooth (e.g., by cutting of corners). In particular, the data modeling problem often occurs in medical imaging. For example, a tumor may be made of the *same* tissue as the organ it is attached to, such that its intensity distribution appears identical to the organ's intensity in the acquired image (meaning that only spatial information can be used to distinguish tumor from healthy tissue). Another example is in the segmentation of heart chambers in which each chamber is filled with blood (i.e., has the same appearance) and, worse, an open valve between the chambers means that only the spatial information is capable of distinguishing one chamber from another. Consequently, in this paper we highlight the ability of our method to operate in these difficult circumstances encountered in medical imaging, with the understanding that the technique could be applied to any arbitrary images encountered in computer vision.

One method which has been used in past to address the unreliability of a data term is to simply employ contrast-dependent *weights* on the graph edges, which requires the optimization of only a single term. However, to avoid a trivial solution, previous methods have employed *seeds*; a foreground seed is a small subset of pixels that have been labeled as belonging to object and a background seed is a small subset of pixels that have been labeled as belonging to background. These seeds may be obtained interactively from a user who is specifying a particular object (e.g., [10,11,12]) or automatically from a system trained to look for a particular object (e.g., [13,14]). For example, this type of approach which uses seeds and contrast-sensitive edge weighting has been employed with such popular algorithms as graph cuts [10], random walker [15], geodesic segmentation [16] and power watersheds [17]. We propose to apply this same approach in the curvature method of [9], which has the effect of allowing object boundary curvature to be high when supported by image contrast, but penalizing boundary curvature for weak or noisy object boundaries. In this way, our formulation solves both of the problems outlined above that can be encountered when a curvature term is used as regularization for a data model, since the formulation does not require a reliable data prior and also permits high-curvature boundaries when supported by data.

The use of a weighted curvature objective function is designed to overcome problems with unreliable data terms and permit a high-curvature object boundary when supported by image contrast. Unfortunately, the authors of [9] perform the optimization of object curvature on a graph using the Quadratic Pseudo-Boolean Optimization with Probing (QPBOP) method, which can be expected to produce *all* unlabeled pixels when there is no unary (data) term [18,19]. Therefore, QPBOP will not allow us to find a global optimum of the weighted curvature functional when no data term is present. However, we show that by introducing an *attraction force* , we can decrease the number

of negative weighted edges in the formulation presented in [9] which allows QPBOP to find the optimal solution.

After describing our image segmentation technique, we demonstrate that it can be applied to control images that were designed to have *zero* difference between the intensity distribution of the object and background, as well as having large sections of missing boundary information. Although other techniques are known for robustness to weak boundaries, such as graph cuts and random walker, we show that they are unable to address these difficult cases, while our algorithm can. Older active contour methods could also be applied to solve some of these image segmentation problems, but they rely on a good initialization and a setting of parameters to tradeoff between multiple terms which often needed to be set individually for each image. Following these control images, our algorithm is applied to a series of medical image segmentation problems that exhibit the same challenges which were observed in the control set.

2   Methods

We begin this section with a review of the 2D curvature optimization framework presented in [9] before proceeding to our contrast weighted curvature formulation, optimization and addition of an attraction force.

2.1   Curvature Energy

The continuous formulation of Mumford's Elastica model is defined for curve $\mathcal{C}$ as

$$E(\mathcal{C}) = \int_{\mathcal{C}} (a + b\kappa^2)ds \quad a, b > 0 \tag{1}$$

where κ denotes the scalar curvature and ds represents the arc length element. When $a = 0$ (the arc length is ignored), the model reduces to the integral of the boundary squared curvature $E(\mathcal{C}) = \int_{\mathcal{C}} \kappa^2 ds$.

The use of combinatorial optimization by [9] to minimize the elastica model prompted the discrete formulation of the curvature on a graph. A graph $\mathcal{G} = \{\mathcal{V}, \mathcal{E}\}$ consists of a set of vertices $v \in \mathcal{V}$ and a set of edges $e \in \mathcal{E} \subseteq \mathcal{V} \times \mathcal{V}$. An edge incident to vertices v_i and v_j is denoted e_{ij}. In our formulation, each pixel is identified with a node, v_i. A weighted graph is a graph in which every edge e_{ij} is assigned a weight w_{ij}. An edge cut is any collection of edges that separates the graph into two sets, $\mathcal{S} \subseteq \mathcal{V}$ and $\overline{\mathcal{S}}$, which may be represented by a binary indicator vector x,

$$x_i = \begin{cases} 1 & \text{if } v_i \in \mathcal{S}, \\ 0 & \text{else.} \end{cases} \tag{2}$$

The cost of the cut represented by any x is given by

$$\text{Cut}(x) = \sum_{e_{ij}} w_{ij} |x_i - x_j|. \tag{3}$$

Bruckstein *et al.* [6] expressed the curvature of a 2D polygon in terms of the angular change between consecutive polygonal segments.

Instead of a polygon, it was observed in [7] that the polygon could be viewed as existing on a *dual* graph. However, in [9] the same idea was formulated on a *primal* graph in order to permit an easier optimization and more generalizable formulation. In this formulation, if two edges e_{ij} and e_{ik}, incident to a node v_i, are cut then the cut is penalized with value $w_{ijk} = \frac{\alpha^p}{min(||\vec{e_{ij}}||,||\vec{e_i k}||)}$, where α is the angle between the edges. This cut penalty was then exactly decomposed into three edge weights

$$E(x_i, x_j, x_k) = w_{ij}|x_i - x_j| + w_{ik}|x_i - x_k| - w_{jk}|x_j - x_k|, \qquad (4)$$

where $w_{ij} = w_{ik} = w_{jk} = \frac{1}{2}w_{ijk}$. Therefore, the minimum cut with respect to these edge weights is a cut that minimizes Bruckstein's discrete curvature formulation on the dual graph. Despite the negative weights, it was shown in [9] that QBPOP was able to find a minimum cut in most circumstances. Notice that although the curvature clique was designed to penalize the cut of both edges e_{ij} and e_{ik}, the decomposition to pairwise interactions add an edge e_{jk} with negative weight. We denote the the set of effective edges with nonzero weights as $\mathcal{E}^* \supseteq \mathcal{E}$.

2.2 Weighted Curvature

To perform curvature based segmentation in [7,9], data term had to be added to the curvature model to obtain the boundary of the object of interest. To solve the segmentation problem without dependence on a data term, we propose to weight the curvature term locally based on the image intensity profile. The primal pairwise curvature formulation in [9] makes it feasible to weight the curvature based on the intensity differences between the terminal points of a particular edge.
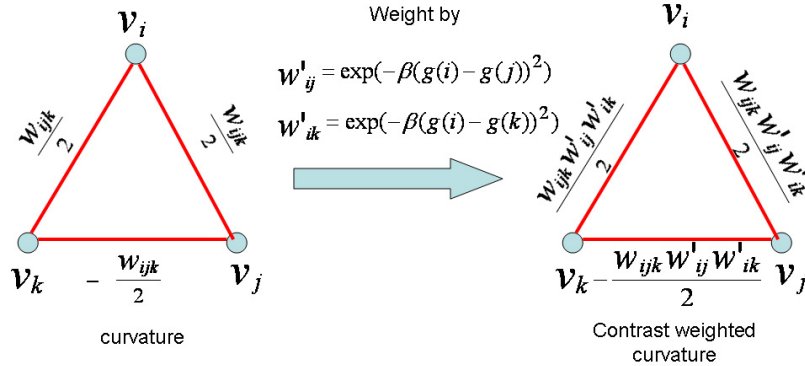
Fig. 1. Weighted curvature clique versus unweighted curvature clique.

According to the curvature formulation in [9], edges e_{ij} and e_{ik} are cut when the pixel i is a foreground pixel and j and k are background pixels or vice versa. Therefore, the curvature clique formed by these edges should be weighted by the intensity differences between pixels i and j and the intensity difference between i and k.

This can be formulated as follows: Given a 2D image with image values associated with each pixel (node), $g : \mathcal{V} \rightarrow R$. The weighted curvature wc_{ijk} is given by

$$wc_{ijk} = w_{ijk} \; w'_{ij} \; w'_{ik}, \tag{5}$$

where

$$w'_{ij} = exp(-\beta(g(i) - g(j))^2), \tag{6}$$

$$w'_{ik} = exp(-\beta(g(i) - g(k))^2). \tag{7}$$

The parameter $\beta \geq 0$ controls the contract strength. The cut penalty is calculated using the same decomposition in 4 with weights $w_{ij}=w_{ik}=w_{jk}=\frac{wc_{ijk}}{2}$ depicted in Figure 1.

The contrast weighted curvature regularization eliminates the dependance on the data model and provides better segmentation of high curvature features in the image (such as sharp corners) when supported by high contrast.

2.3   Optimization

In the previous sections, the original Bruckstein formulation of polygonal curvature was transformed into the problem of finding a minimum cut on a graph in which some of the edge weights were negative. Unfortunately, the negative edge weights introduced by the third term of (4) causes the minimum cut problem to be nonsubmodular [20], *i.e.*, straightforward max-flow/min-cut algorithms will not yield a minimum cut. However, it was shown in [9] that the Quadratic Pseudo Boolean Optimization (QPBO) [18] and Quadratic Pseudo Boolean Optimization with Probing (QPBOP)[19] offered a solution to the optimization problem that frequently offered a complete, optimal solution.

A practical problem that we encountered due to the elimination of the data model (unary term or terminal links in the graph) is that the optimization using QPBO/ QPBOP (used in [9]) fails to provide complete labeling. Hence, in the next section present the *attraction energy* that enables the QPBO/ QPBOP to provide complete labeling.

2.4   Attraction Energy

The second contribution of this paper is the introduction of the attraction force to the segmentation problem. The attraction force is inspired by the intermolecular forces that maintain the structure of the molecule and prevent it from decomposing into its salient atoms. This scenario is very analogous to the segmentation problem where the object to be segmented is similar to a molecule that we would like to maintain its atoms (the pixels that constitute the object of interest) tightly connected to each other. Coulomb's Law states that the force of attraction between two objects is equal to the product of their charges q_1 and q_2 is given by

$$F = \frac{k}{r^2} q_1 q_2, \tag{8}$$

where k is the Coulomb's constant and r is the distance between q_1 and q_2. Hence in our discrete formulation, we need to maximize the attraction force between two variables

x_1 and x_2 given by

$$E_{\text{attraction}} = \frac{w_{12}}{2}(x_1 x_2 + (1 - x_1)(1 - x_2)^1), \tag{9}$$

where w_{12} is the weighted curvature weight of the edge e_{12} described in the previous section. Notice that maximizing this attraction force is equivalent to minimizing its negative.

A key value of the attraction force is that it allows for an optimization of the curvature energy in the absence of the unary term. Specifically, the construction in [20] represents the negative attraction energy by adding edges e_{12} with weight w_{12}, $e_{\mathcal{S}1}$ an edge $e_{2\mathcal{T}}$ with weights $\frac{w_{12}}{2}$. The addition of positive weights changes the sign of some of the negative weights introduced by the curvature term. This justifies our choice for the attraction weight as $\frac{w_{12}}{2}$ which makes the the weight of e_{12} nonnegative. These sign changes affect the optimization problem by strongly decreasing the number of unlabeled variables in the output of the QPBOP.

2.5   Summary

The segmentation problem is modeled as the solution, x, which minimizes the energy

$$E(x) = E_{\text{curvature}}(x) - \lambda \, E_{\text{attraction}}(x), \tag{10}$$

for strictly positive weighting parameter λ that controls the relative importance of the attraction energy with respect to the curvature energy.

The curvature term is written as a summation by

$$E_{\text{curvature}}(x) = \sum_{e_{ij} \in \mathcal{E}^*} w_{ij}|x_i - x_j|, \tag{11}$$

and the attraction force is given by

$$E_{\text{attraction}}(x) = \sum_{e_{ij} \in \mathcal{E}^*} \frac{w_{ij}}{2}(x_i x_j + (1 - x_i)(1 - x_j)). \tag{12}$$

Foreground and background seeds are used to initialize the segmentation, a foreground seed v_i is set to $x_i = 1$ while a background seed would be set to $x_i = 0$.

3   Experimental Results

This section presents a sample of our segmentation results using weighted curvature and compares our segmentation to the corresponding results obtained by graph cuts and random walker. In all of our results, we have used the 8-point connected lattice.

---

[1] Note that the addition of the second term here is very natural and still analogeous to (8) in the sense that we have two molecules, one for the foreground and one for the background and hence we have to add two terms for the attraction force; one penalizing both pixels to be labeled 1 and another to penalize both pixels being labeled 0

We begin by demonstrating the usefulness of weighted curvature on synthetic images. These synthetic images feature two important challenges that can only be resolved by weighted curvature regularization: 1) Absence of data differences at some parts of the boundary, *i.e.*, object and background have the same intensity profile. 2) Segmentation of high curvature features such as cusps and sharp corners.

Figure 2 shows three images that the human visual perception can seamlessly define where the boundaries of objects of interests are. However, some of the most advanced segmentation tools can not. For example, in the first image of Figure 2, it is obvious that the blue seed should provide an object that ends where the white lines end. Graph cuts favor the cut with the minimal number of edges since there no contrast between the neighboring pixels which yields a trivial solution isolating the blue seed as a foreground and the rest of the image as a background, graph cuts also gave trivial solutions in the rest of the images. Random walker works, intuitively, by calculating the probability that a random walk starting at a particular pixel will first reach one of the seeds. Hence, it suffers from a proximity problem that results in a premature stopping and segments a bar with a smaller length than the correct one. Our approach provides the correct segmentation. Although the seed is very far from the end of the bar, our algorithm could extend the segmentation until the end of the bar. This is simply because a a straight line has a minimal curvature so the algorithm extends the bar until an intensity difference occurs.

The second image features a disconnected boundary. This challenge is common in real images when acquisition artifacts such as noise and occlusion disconnect the boundary. In medical images, anatomical abnormalities such as stenosis in vessels may cause the boundary to appear disconnected. The random walker leaks through these gaps and fails to separate the object from the background correctly. Weighted curvature, however, succeeds to bridge the gaps in the boundary due to the unique ability of curvature to preserve object continuity as connected boundaries have less curvature than disconnected ones. Meanwhile, the sharp corners were not smeared by curvature minimization because they were supported by contrast and the curvature is weighted by this contrast information in our formulation. The third image consists circle with a bump (of the same intensity) attached to it. The large circle is the object of interest that should be separated from the smaller bump and the black background. This scenario is very common in medical images. For example, a tumor may be made of the same tissue as the organ it is attached to, with no intensity differences between the tissue and the tumor (see Figure 6) or two proximal distinct structures may have the same intensity profile (such as the caudate and the putamen in brain MRI, for example). In figure 2, random walker stops prematurely yielding a smaller circle than the correct one because a random walk from an erroneously-background-labeled pixel would have a higher probability reaching the background seeds than the foreground one. However, weighted curvature succeeds to obtain the correct boundary; the contrast based weights forces the boundary to stop when it hits a black pixel isolating the large circle from the background. And the curvature favors a circle with larger radius and hence it extends the foreground seeds until it reach the boundary between the large circle and the smaller bump. The foreground can not be extended any further, otherwise, it would form a cusp at the blue seed in the bump yielding a high curvature. Premature segmentation is pro-
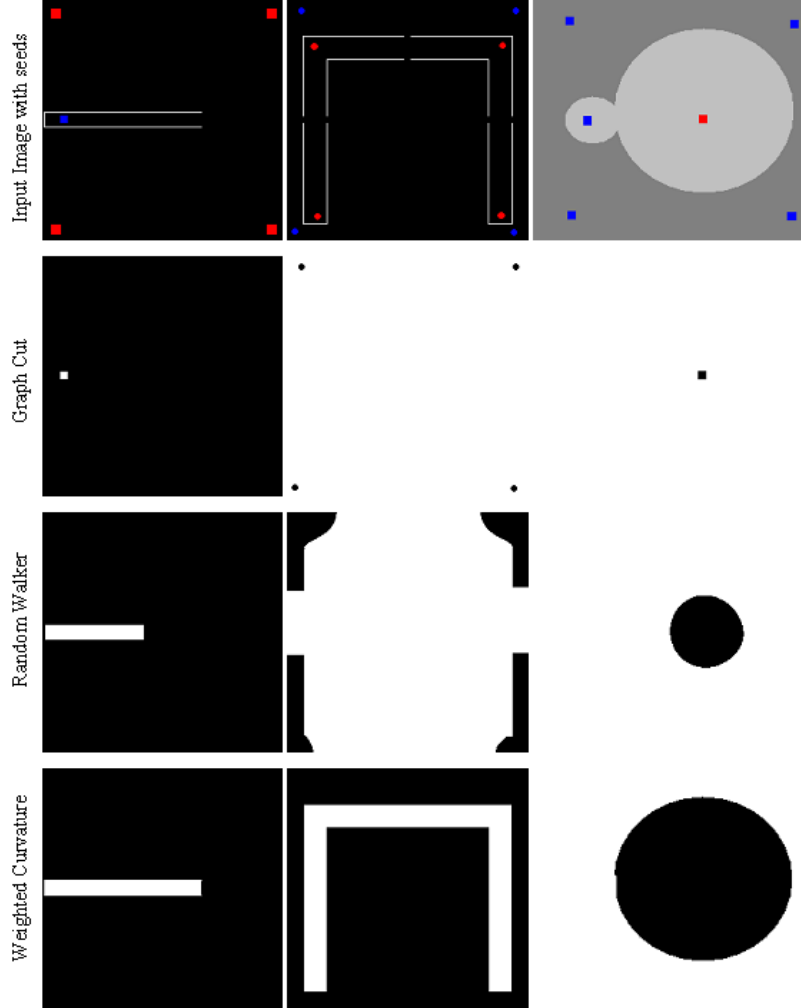
Fig. 2. Segmentation of some challenging images. Graph cuts provide a trivial solution by isolating the foreground or the background seeds. Random walker suffers from proximity problem that yields a smaller object than the desired in images 1 and 3. It also suffers from a leakage producing a segmentation of the second image due to the gaps in the boundary. Weighted curvature extends the bar in the first image at no cost and stops when contrast change occurs. It bridges the gaps in the second image because curvature preserves connectivity. In the third image, the curvature regularization separates two structures of the same intensity.

hibited by the fact that a circle with a larger radius has a smaller curvature than a circle with a smaller radius. Figure 3 shows similar examples with larger gaps in the boundaries. Notice that although the gaps in the dotted curve (in the first image) are very
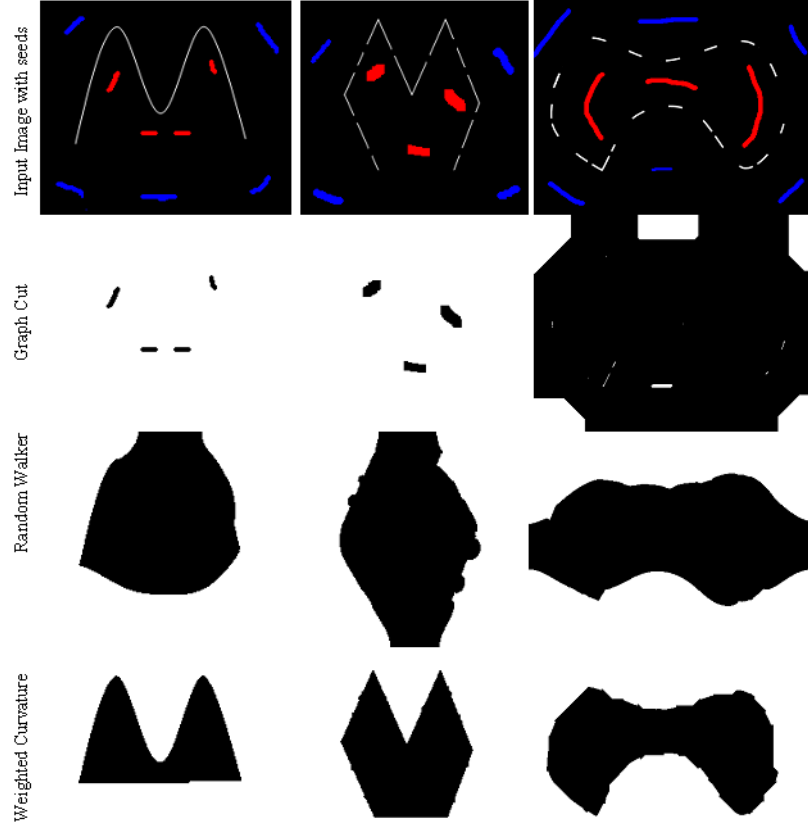
Fig. 3. Segmentation of boundaries with very large gaps and zero contrast between foreground/background pixels. The gaps caused leakage in the random walker that failed to provide the desired segmentation. Curve continuity is promoted by curvature regularization that enables our approach to bridge the gaps in the boundaries of the three images. Our approach also maintains the cusps in the first two images because they are warranted by the contrast weighted edges.

small, these gaps caused the random walker to leak. Also, random walker could not connect the large gap, between two end points of the curve, by a straight line. Weighted curvature, however, prefers the straight line because of its minimal curvature which wields the desired segmentation. The second and third images in Figure 3 also feature very large gaps in the boundaries with no foreground/background contrast, these gaps challenged the random walker resulting in erroneous segmentation. Weighted curvature succeeds to bridge all the gaps in the boundaries. Notice that the cusps in the first image and the sharp corners in the second image were segmented correctly because the curvature weights are contrast dependent.

The previous challenges occur frequently in medical images. Here we demonstrate the performance of our model on several medical imaging applications and different
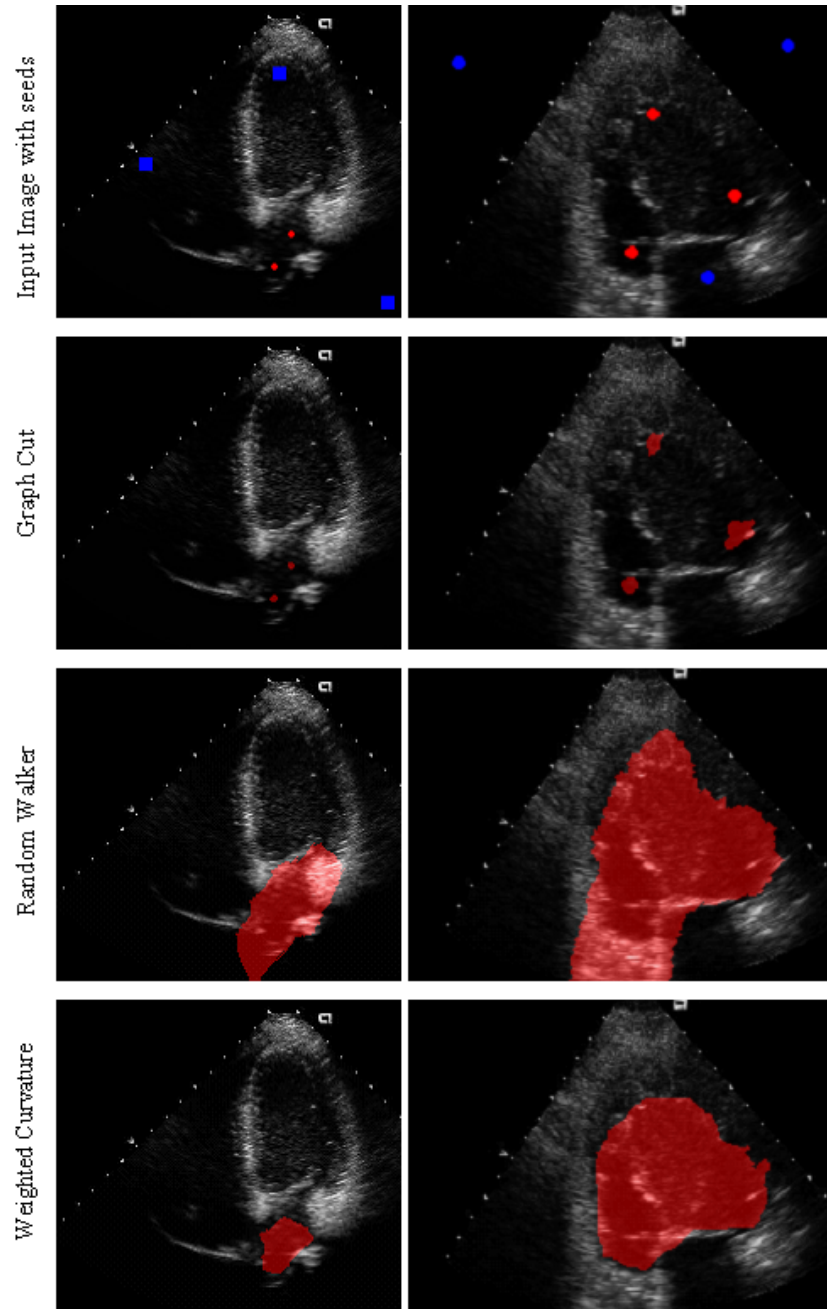
Fig. 4. First column: Segmentation of the left Atrium. Second Column: Segmentation of the left ventricle. Graph cuts yielded a trivial segmentation around the seeds. The lack of contrast between the left atrium and the background, in addition to the proximity of several parts of the images to the foreground seeds forced the random walker to leak and produce an overcompensation of the region of interest in both cases. Weighted curvature prevented leakage because leakage introduces higher curvature cost of the boundary.
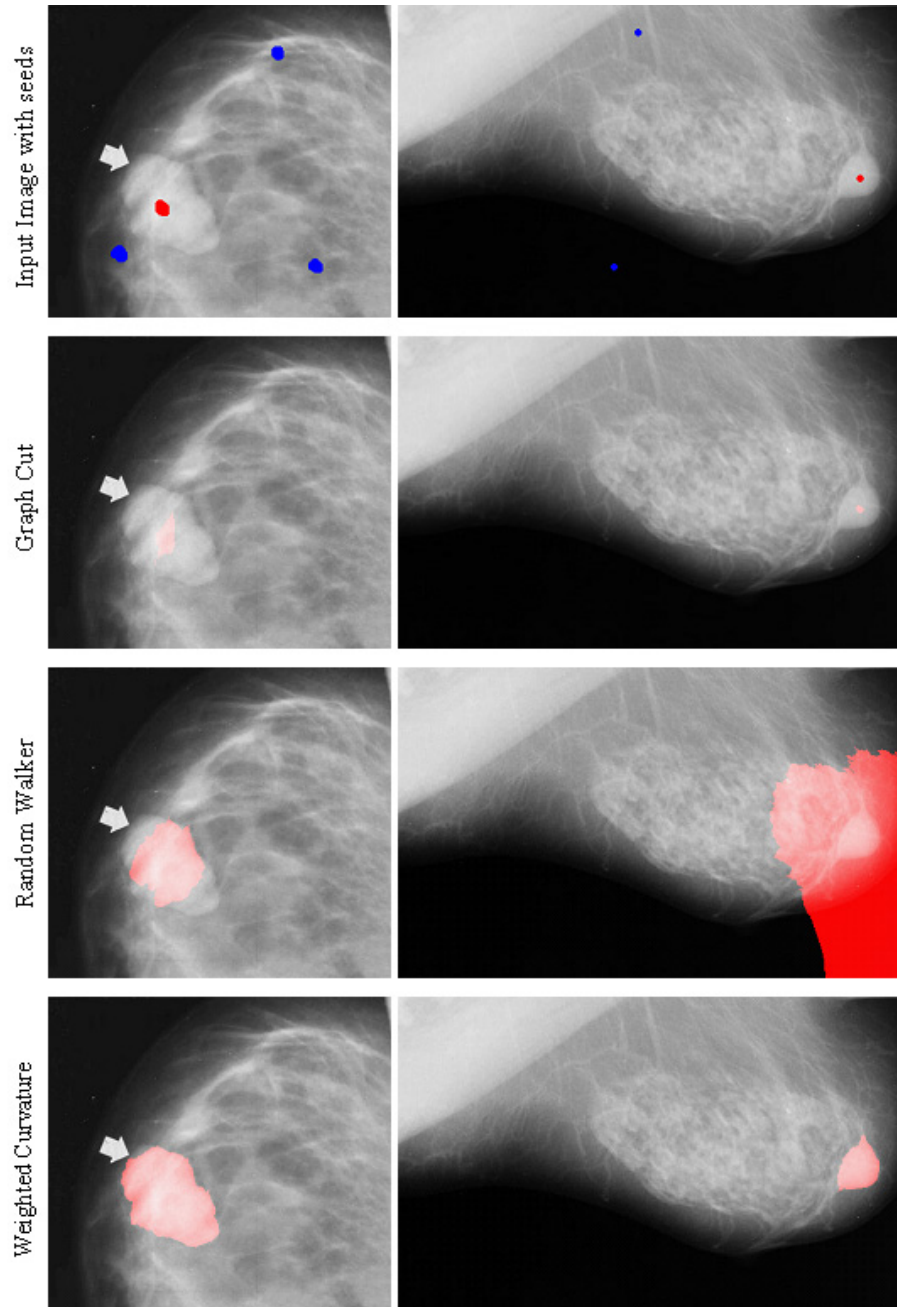
Fig. 5. Segmentation of circumscribed masses in mammograms. Graph cuts resulted in a trivial solution by cutting the edges around the foreground seeds. Random walker resulted in false negatives in the segmentation of the first mass and false positives in the segmentation of the second one because the probability of a random walk reaching a foreground or background seed is affected by the location of the seeds yielding a false segmentation in both cases. Weighted curvature detected the correct boundaries in both cases.
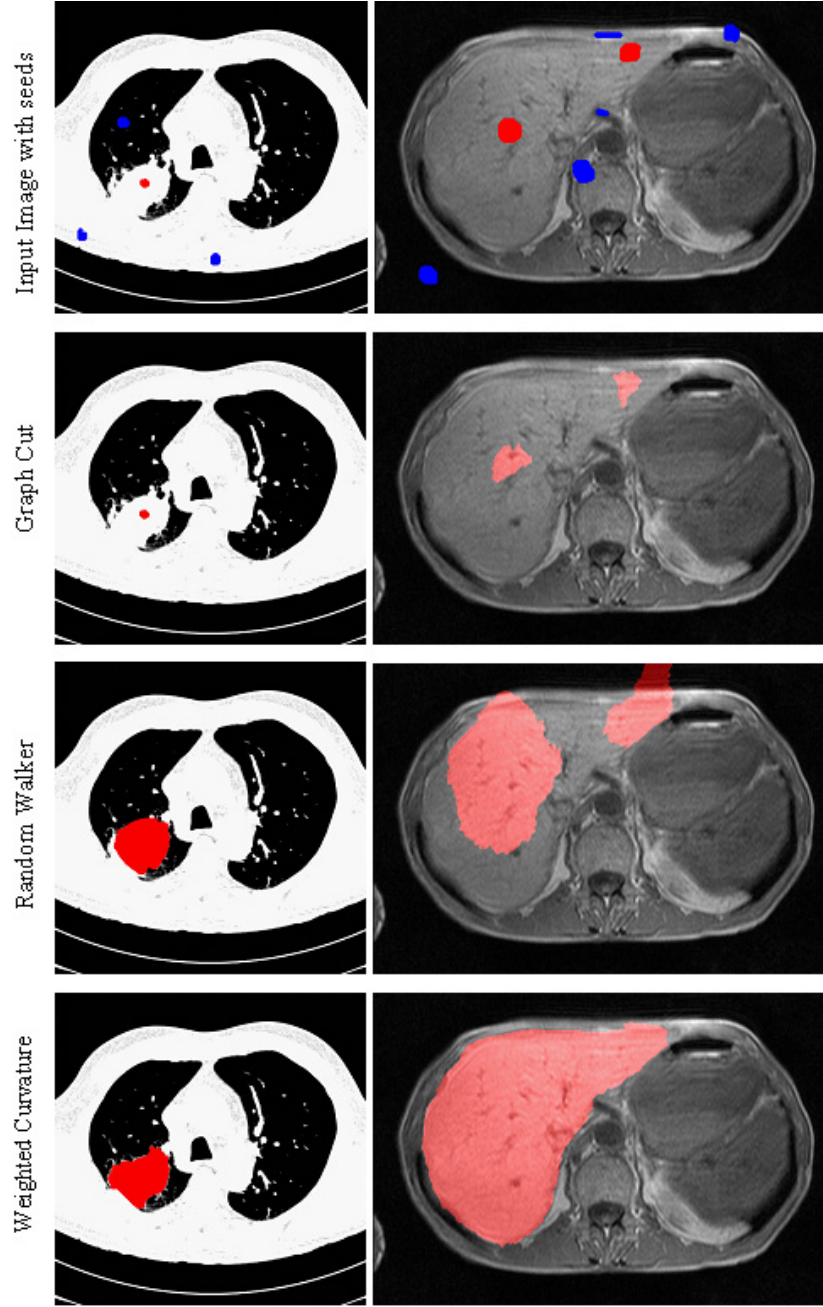
Fig. 6. First column: Segmentation of a lung tumor in a chest CT scan. Graph cuts produced a trivial segmentation around the foreground seed. Random walker did not extract the whole tumor due to the proximity of some tumor pixels to background seeds. Weighted curvature correctly classified the pixels that random walker missed due ti their high contrast with the lung tissue. Second column: segmentation of the liver in an abdominal MRI slice. Random walker yielded false positives and false negatives and disconnected the liver into two pieces while weighted curvature preserved the connectivity of the liver and captured the correct boundary.

modalities. Figure 4 shows the segmentation of the left atrium in ultrasound. The atrium has the same intensity profile as the rest of the heart chambers and the background with no clear boundaries. Graph cuts yielded a trivial solution isolating the foreground seeds as the object and the rest of the image as a background. The absence of image contrast between the atrium and the background resulted in an over-segmentation by random walker. The segmentation using our proposed approach succeeded to extract the left atrium correctly. The second columns of Figure4 exhibits another example for such challenges where the left ventricle is the object to be segmented. Mass segmentation in mammograms is a challenging problem that can not easily be modeled by data terms because of the large variability among the different types of breast tissues (e.g fatty, glandular and dense tissues) and because of the variability in the appearance and shape of the masses . Figure 5 demonstrates the segmentation of two circumscribed masses in mammograms. For the first mass, the random walker result suffers from false negatives (under-segmentation) while the second mass the random walker provided false positive pixels (over-segmentation). In both cases, the weighted curvature yielded a correct segmentation. Figure 6 depicts the segmentation of a lung tumor in a chest CT scan. There is no contrast between the tumor and abdominal muscles. Random walker stopped prematurely (due to the proximity issue) and did not extract the whole tumor while our segmentation did. The weighted curvature expands the foreground minimize the curvature of its boundary and it stops when it reaches the boundary between the tumor and the muscles that produces the least curvature. The second column of figure 6 shows a similar case where there is no contrast between the liver and the abdominal muscles in an abdominal MR scan. Random walker yielded some false positives and and false negatives. For example, the upper boundary of the liver was disconnected by random walker. It is intuitively clear that random walks starting at these erroneously-background-labeled pixels (the gap between the two pink parts captured by random walker) have higher probability to reach background seeds than foreground and hence falsely labeled as background. However, curvature regularization favors a smooth boundary over a disconnected one because disconnecting the upper boundary into two pieces would form corners with high curvature. All the previous results were obtained using the same parameters for attraction force and contrast weighting. Complete global solution was obtained in each case. The addition of the attraction force enabled the QPBO to provide complete labeling without any need to perform probing which makes our algorithm even faster than [9]. In the few cases that QPBO did not label all the pixels, the probing was able to provide these pixels yielding a global optimal solution.

4   Conclusion

We proposed an image segmentation method which isolates an object boundary by using weighted curvature. Weighted curvature allows us to segment an object in challenging situations in which a data term is unreliable or missing, as is common in medical image segmentation tasks. Additionally, our formulation of weighted curvature permits the segmented object boundary to exhibit a high curvature if it is warranted by the image data. The inclusion of an attraction force allows us to find a global optimum of the model using QPBOP in a few seconds.

Our experiments demonstrate that our model can be used to complete object boundaries in controlled experiments where the object/background shared the same intensity distribution and significant parts of the boundary were missing. In contrast, other leading algorithms which are known for this type of robust behavior were unable to achieve segmentations of these challenging control images. Similarly, our algorithm was demonstrated to provide quality segmentations on image segmentation tasks appearing in medical images which exhibit similar challenges to the control images. Once again, we demonstrate that graph cuts and random walker are unable to perform with such little information (in terms of image data and seed numbers/placements). In all of these experiments, both control and real, the *same* parameters were used for the contrast weighting and attraction force term.

Future work will be to investigate the use of other optimization methods that might allow us to remove the attraction force (and consequent parameter), the use of a data term in conjunction with weighted curvature and to take advantages of recent advances in GPU-based graph cuts (and therefore QBPOP) to further accelerate the already fast speed of our method.

References

1. Mumford, D.: Elastica and computer vision. Algebriac Geometry and Its Applications (1994) 491–506
2. Kass, M., Witkin, A., Terzopoulos, D.: Snakes: Active contour models. International Journal of Computer Vision **1** (1987) 321–331
3. Caselles, V., Kimmel, R., Sapiro, G.: Geodesic active contours. IJCV **22** (1997) 61–79
4. Shen, J., Kang, S.H., Chan, T.F.: Euler's elastica and curvature-based inpainting. SIAM Journal of Applied Mathematics **63** (2003) 564–592
5. Esedoglu, S., Shen, J.: Digital inpainting based on the mumfordshaheuler image model. European Journal of Applied Mathematics **13** (2002) 353–370
6. Bruckstein, A., Netravali, A., Richardson: Epi-convergence of discrete elastica. Applicable Analysis **79** (2001) 137–171
7. Schoenemann, T., Kahl, F., Cremers, D.: Curvature regularity for region-based image segmentation and inpainting: A linear programming relaxation. In: ICCV, Kyoto, Japan (2009)
8. Schoenemann, T., Cremers, D.: Introducing curvature into globally optimal image segmentation: Minimum ratio cycles on product graphs. In: ICCV. (2007) 1–6
9. El-Zehiry, N., Grady, L.: Fast global optimization of curvature. In: Proc. of CVPR. (2010)
10. Boykov, Y., Jolly, M.P.: *Interactive graph cuts* for optimal boundary & region segmentation of objects in N-D images. In: Proc. of ICCV. (2001) 105–112
11. Rother, C., Kolmogorov, V., Blake, A.: "GrabCut" — Interactive foreground extraction using iterated graph cuts. In: Proc. of SIGGRAPH. Volume 23., ACM (2004) 309–314
12. Grady, L., Schiwietz, T., Aharon, S., Westermann, R.: Random walks for interactive organ segmentation in two and three dimensions: Implementation and validation. In Duncan, J., Gerig, G., eds.: Proceedings of MICCAI 2005. Number 2 in LNCS 3750, Palm Springs, CA, MICCAI Society, Springer (2005) 773–780
13. Funka-Lea, G., Boykov, Y., Florin, C., Jolly, M.P., Moreau-Gobard, R., Ramaraj, R., Rinck, D.: Automatic heart isolation for CT coronary visualization using graph-cuts. In: Proc. of ISBI. (2006) 614–617
14. Wighton, P., Sadeghi, M., Lee, T.K., Atkins, M.S.: A fully automatic random walker segmentation for skin lesions in a supervised setting. In: Proc. of MICCAI. (2009) 1108–1115

15. Grady, L.: Random walks for image segmentation. IEEE Trans. Pattern Anal. Mach. Intell. **28** (2006) 1768–1783
16. Bai, X., Sapiro, G.: A geodesic framework for fast interactive image and video segmentation and matting. In: Proc. of ICCV 2007, Rio de Janeiro, Brazil, IEEE (2007)
17. Couprie, C., Grady, L., Najman, L., Talbot, H.: Power watersheds: A new image segmentation framework extending graph cuts, random walker and optimal spanning forest. In: Proc. of ICCV. (2009) 731–738
18. Kolmogorov, V., Rother, C.: Minimizing nonsubmodular functions with graph cuts — A review. IEEE Trans. Pattern Anal. Mach. Intell. **29** (2007) 1274–1279
19. Rother, C., Kolmogorov, V., Lempitsky, V.S., Szummer, M.: Optimizing binary MRFs via extended roof duality. In: Proc. of CVPR. (2007)
20. Kolmogorov, V., Zabih, R.: What energy functions can be minimized via graph cuts? IEEE Trans. Pattern Anal. Mach. Intell. **26** (2004) 147–159